INCREASING THE CAPACITY OF A LANE-FREE BELTWAY FOR CONNECTED AND AUTOMATED VEHICLES USING POTENTIAL LINES

Majid Rostami-Shahrbabaki, Corresponding Author
Chair of Traffic Engineering and Control, Technical University of Munich
Arcisstrasse 21, 80333 Munich, Germany
majid.rostami@tum.de
ORCiD: 0000-0002-8129-4519

Hanwen Zhang
Chair of Traffic Engineering and Control, Technical University of Munich
Arcisstrasse 21, 80333 Munich, Germany
hanwen.zhang@tum.de
ORCiD: 0000-0001-9051-3894

Maya Sekeran
Chair of Traffic Engineering and Control, Technical University of Munich
Arcisstrasse 21, 80333 Munich, Germany
maya.sekeran@tum.de
ORCiD: 0000-0002-5508-8463

Klaus Bogenberger
Chair of Traffic Engineering and Control, Technical University of Munich
Arcisstrasse 21, 80333 Munich, Germany
klaus.bogenberger@tum.de
ORCiD: 0000-0003-3868-9571

Word Count: 5612 words + 0 table(s) × 250 + 500 words in references = 6112 words

Submission Date: December 7, 2022

ABSTRACT
Road congestion implies that there is not enough capacity to meet the demands of road users. One solution to increase traffic network capacity is to build beltways. A beltway guides commuters to use alternative routes without entering the city core. However, this approach has led to urban sprawls causing extended land use and induced traffic demand. Recent developments in automated vehicles with communication capabilities allow us to re-think traffic systems by optimizing current road infrastructure leading to the idea of lane-free traffic (LFT). LFT removes lane marking and allows vehicles to exploit the entire road's width, increasing lateral occupancy and reducing congestion on the beltways. In this paper, we introduce a new approach using potential lines for a CAV's driving strategy that significantly increases the capacity of a lane-free beltway. Potential lines are described as a method to laterally organize the CAVs on a beltway based on their desired speeds. Compared to other available lane-free driving strategies, this approach reduces lateral interaction and maneuvers, leading to much higher throughput. The results show that the critical density of the considered beltway can reach up to 250 veh/km with a maximum flow of 27036 veh/h, which is almost four times of a similar lane-based beltway. These promising results render more road construction or road extensions obsolete. Additionally, with the proposed idea, the width of the existing roads can be reduced, and the extra capacity can be allocated to other road users.

Keywords: beltway, ring road, lane-free traffic, potential lines, connected and automated vehicles (CAVs)

INTRODUCTION

There are two ways by which traffic network capacity can be increased - building more roads or using innovative traffic management approaches to maximize the exploitation of the current road capacity. The first approach often leads to costly investments, while the second approach may work for the short term as it caters to current traffic demand unless the long-term demand can be controlled. The number of auto vehicles on the road exploded over the years, especially after World War II. To address this huge demand, modern roads were introduced to manage traffic congestion and to better connect different places on land. This includes introducing beltways (also referred to as ring roads). Beltways are constructed with the aim of decentralizing urban areas and reducing congestion within the radius of highly dense cities by offering alternative routes for vehicles instead of entering the city core. However, the issue remains with the increasing number of cars on the road but still not enough road networks to meet this demand despite continuous road infrastructure developments.

From the construction design aspect, beltway attributes towards a displacement of service sector and industrial activities (*1, 2*). This, in turn, reduces city population by 20% through moving jobs and housing away to suburban areas. In Beijing, there are currently seven ring roads but yet no sign of relief for traffic congestion and carbon emission (*3*). A case study on the big Almaty ring in Kazakhstan shows that ring roads are good for short-term congestion relief but not sustainable in the long run (*4*) as also observed in other cities around the world (*4, 5*). The effect is a significant increase up to 20% in traffic after only one year. It is not surprising to observe that the forecast for traffic intensity does not include induced traffic as a factor since the economical benefits outweigh the congestion and travel time factors. An earlier case study on a beltway in Virginia in 1958 already showed adverse effects on the reduction of road capacity (*5*). These developments also causes environmental impacts such as deforestation and displacement of wildlife to make way for road expansions (*6–8*).

To manage ongoing capacity drop on beltways, traffic planners/controllers started using technology through the implementation of intelligent traffic systems (ITS) (*9–11*). However, despite these attempts, capacity drop on beltways remains a problem. Therefore, the question remains, how do we increase traffic capacity on current beltways and optimize existing road infrastructure? A beltway typically has between four to six lanes (two or three lanes in each direction). The width of the lanes is maximized for large vehicles. Therefore the common car typically occupies about 50% of a lane width. This fact indicates that, laterally, a three-lane beltway could theoretically span roughly six cars instead of three cars. But this is not doable with current lane-based traffic system with predefined lane markings. Even the lane detection and lane-keeping assistant algorithms in automated vehicles (AVs) will force the vehicles to adhere to lane rules. Although driving in lanes aid human drivers to focus on the traffic ahead and to ensure some level of traffic safety, it becomes complex and risky when human drivers perform lane changes that requires multiple angles of perception before performing a lateral move. This causes inefficient driving that often leads to accidents while also limiting dynamic road capacity.

From an infrastructure standpoint, developing more beltways will be unsustainable as it also involves long-term and costly maintenance of road markings and road signs. Furthermore, there have been discussions about how AVs will deal with faded lane marking over the years. All the issues mentioned so far leads to the following research question - what if we do away with lane-markings and corresponding road signs by introducing lane-free traffic on roads? This can be made possible by leveraging CAV capabilities equipped with advanced sensors, vehicle to vehicle (V2V) communications and efficient control algorithms. With these capabilities, it opens up opportunities for new traffic systems that allows for vehicles to move seamlessly through traffic in a lane-free manner with communication updates between vehicles and the infrastructure to guide the traffic systems.

Lane-free traffic is a new and futuristic idea, and in order to realize lane-free traffic with CAVs, there is potential to re-think traffic design. The earliest work found so far is by (*12*) with the idea of rendering the lane markings obsolete and allowing the vehicles to drive on a continuous 2-d surface, more specifically, along any desired lateral location of the road. The term lane-free traffic was first coined in a point of view paper by Papageorgiou et al. (*13*). The authors suggested two combined principles for LFT namely "lane-free" traffic and "nudging". The first principle allows vehicles to be at any lateral position within the road boundary. While "nudging" is inspired by the effect of fast-moving vehicles on the front slower vehicles in a lane-less traffic observed in some countries with low lane discipline. These faster vehicles apply a pushing force by honking the vehicles in front to make space for overtaking. This new force implies that the upstream vehicles can impact downstream vehicles. This impact is not represented in conventional traffic flow models. Figure 1 below shows the concept of LFT compared to lane-based traffic.

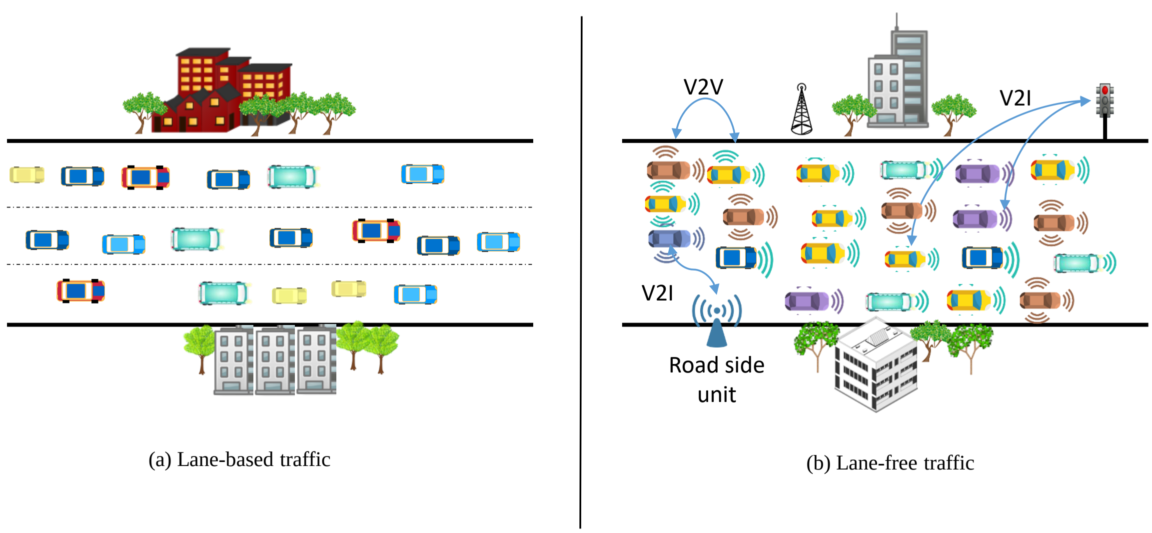

(a) Lane-based traffic (b) Lane-free traffic

FIGURE 1: Lane-based traffic vs Lane-free traffic (*14*)

Since then, several control designs have been proposed considering both classical and advanced approaches for deriving strategies in the LFT. In this paper, we introduce the concept of potential lines to uniformly assign the lateral occupancy of the road based on the desired speed of the vehicles. This novel approach extensively increases the traffic capacity on lane-free beltways. Furthermore, we consider the factor of large differences in speed that causes faster vehicles to move in slalom. Potential lines prevent this by reducing lateral interaction and maneuvers thus increasing traffic safety as well. To the best of our knowledge, this approach has not been considered before. The research in (*13, 15, 16*) shows that the capacity of a freeway with three lanes that is generally about 6000-7000 veh/h would increase to 14000-15000 veh/h in the lane-free condition, doubling the current lane-based capacity. However, with the developed potential lines, the achieved flow in the ring road is almost four times of equivalent the lane-based road.

LITERATURE REVIEW

To manage capacity drop on beltways, innovative solutions using technology were introduced. In (*17*) a dynamic speed control strategy increases capacity and speed but only if there are policies in place to control demand. In (*18*), the authors proposed separating lane usage based on class of vehicles. However, this approach may lead to under use or over use of certain lanes. In (*19*), the authors proposed a beltway feedback strategy that may be implemented as a feedback system for CAVs while not requiring lane-based adherence. To manage the increasing traffic congestion along the Venice-Mestre area despite the introduction of the MARCO system, project MARCO-T3 installed several traffic management mechanisms (*9*). Among these are traffic monitoring, video surveillance, automatic incident detection (AID), ramp metering, variable message sign (VMS), lane control sign (LCS), textual information and rerouting, and multiagency incident management (MIM). An evaluation conducted eight years later show a reduction of congestion hours by 21%. However, there was no indication of the cost to maintain this integrated system. The risk of one or more of the systems failing at any point could also cause issues where the traffic can no longer be managed for a certain period of time. The I-66 Beltway in the United States introduced a dynamic tolling system that benefited alternative route travel time but not in the opposing direction of the beltway during tolling hours (*10*). Another approach is to implement ramp metering as described in (*11*) where over 10 different ramp metering algorithms are implemented on various freeways in the United States.

As mentioned earlier, lane-free traffic is a new concept for a fully automated traffic environment. Therefore there is potential to design new vehicle driving strategies for CAVs to increase road capacity. Recent studies introduce several classical approaches to control vehicle movements in LFT. In (*20*), the authors proposed an optimal path planning algorithm using nonlinear Optimal Control Problem (OCP) for efficient vehicle advancement. In Levy and Haddad (*21*) applied the non-linear MPC framework to plan the trajectories of the vehicle in order for the vehicles to self-advance with minimal control. Decentralized controllers as proposed in (*22*) ensures safety of vehicle operations in LFT. Other advanced controllers uses reinforcement learning (*15*) and coordination graphs (*16*) to facilitate collaborative multi-agent decision making.These work show that the capacity of the lane-free road can be almost doubled compared to the similar lane-based road.

To further increase road capacity, especially on beltways or highways, barriers that separates bi-directional traffic can also be removed to allow vehicles to share the total road width. A flexible and dynamic internal boundary as explored in (*23*) and (*24*) is introduced which help to serve asymmetric traffic demands. In Chavoshi and Kouvelas (*25*), the authors proposed a distributed controller within clusters of vehicles. The non-linear MPC is applied to control the movement of vehicles in each cluster. Other approaches such as vehicle flocking also have potentials for increasing road capacity (*26*).

These strategies show promising ways by which LFT systems can be implemented to increase road capacity. In this work, we introduce the idea of potential lines which allows for the uniform lateral distribution of the vehicles based on their desired speed. This approach leads to much higher flow rates mainly due to removing unnecessary lateral movement of vehicles. In the following section, our proposed methodology is elaborated.

METHODOLOGY

The proposed methodology consists of four parts: 1- a cruise controller allowing vehicles to reach their desired speed; 2- artificial potential fields for collision avoidance, and, most importantly, 3-

potential lines for uniform lateral distribution of the vehicles across the road width. In addition, 4- a boundary controller is implemented which keeps the vehicles within the road boundary by constraining the lateral accelerations. The implementation of the potential field is the main novelty of this present work which leads to significantly high throughput. In the following subsections, first, the considered vehicles dynamics is explored, then the details of the proposed approach are given.

Vehicle dynamics

For the movement of the vehicles in the lane-free environment, we used the double integrator model to describe the vehicle dynamics. The discrete-time differential equations are used where T is the sampling period and $k = 0, 1, \ldots$ is the discrete time index where $t = k \cdot T$. For a given vehicle i, the vehicle dynamics is described with the following state-space equations in the longitudinal and lateral directions:

$$x_{1,i}(k+1) = x_{1,i}(k) + Tx_{2,i}(k) + \frac{1}{2}T^2 u_{x,i}(k) \tag{1a}$$

$$x_{2,i}(k+1) = x_{2,i}(k) + Tu_{x,i}(k) \tag{1b}$$

$$x_{3,i}(k+1) = x_{3,i}(k) + Tx_{4,i}(k) + \frac{1}{2}T^2 u_{y,i}(k) \tag{1c}$$

$$x_{4,i}(k+1) = x_{4,i}(k) + Tu_{y,i}(k) \tag{1d}$$

where $x_{1,i}$ and $x_{2,i}$ are the longitudinal position and speed of the vehicle whereas $x_{3,i}$ and $x_{4,i}$ represent lateral position and speed, and $u_{x,i}$ and $u_{y,i}$ are longitudinal and lateral accelerations, respectively. Note that the vehicle states are measured with respect to the vehicle's center. The motion dynamics (Equation 1) are subject to the following bound constraints.

$$-u_{x,min} < u_{x,i}(k) < u_{x,max} \tag{2a}$$

$$-u_{y,min} < u_{y,i}(k) < u_{y,max} \tag{2b}$$

The longitudinal and lateral acceleration of vehicles are limited due to the physical capability of the vehicles for accelerating, braking, steering, and of course due to the comfort issues of the passengers. Such accelerations are defined based on two main forces applied to each vehicle; target speed and inter-vehicle forces. The target speed force is induced via a cruise control loop as the result of the vehicle's desire to drive at its desired speed. On the contrary, the inter-vehicle force induced by an artificial potential field around each vehicle prevents collision among vehicles. The inter-vehicle force comprises a nudging force applied to the front vehicle and a repulsive force applied to the following vehicle. In addition, a lateral force is applied to the vehicle based on the proposed potential lines. The details on how each force is calculated are given in the following subsections.

Cruise controller for achieving desired longitudinal speed

One goal in designing driving strategies for CAVs in the lane-free environment is to allow them to drive as closely as possible, whenever possible, to their desired speed. To this end, a cruise controller with a target speed set-point is used. The longitudinal target speed $v^{ts}_{x,i}$ is defined as the minimum of the vehicle desired speed $v^{d}_{x,i}$ and a multiple of its current speed as $min\left\{1.3 \times x_{3,i}(k), v^{d}_{x,i}\right\}$. This allows for a smooth increase in the vehicle speed and less desire to accelerate during the congestion. Note that the longitudinal desired speed of the vehicle may differ from one vehicle to the other, whereas, for comfort and safety reasons, the desired lateral speed of each CAV is zero. A feedback P-controller (Equation 3) is used as the cruise controller to regulate the longitudinal speed of the vehicles using the target speed forces $f^{ts}_{x,i}$ as follows:

$$f^{ts}_{x,i}(k) = k^{ts}_x(v^{ts}_{x,i} - x_{3,i}(k)) \tag{3}$$

where k^{ts}_x and k^{ts}_y are controller gains. As just mentioned, the lateral target speed is zero. The implemented cruise controller is shown in Figure 2 for regulating the longitudinal speed. The lateral speed is controlled using the potential lines and will be explained later.

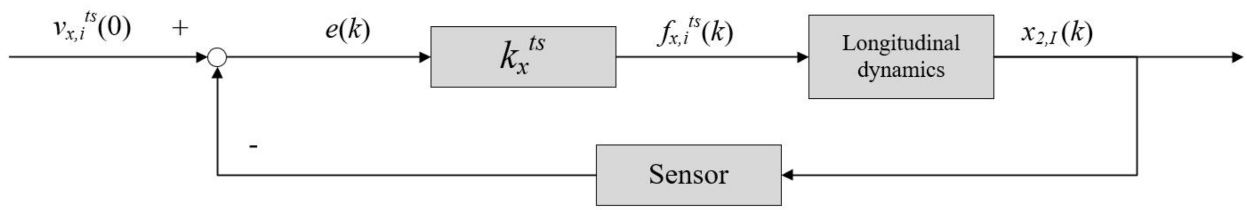

FIGURE 2: Feedback loop for the cruise controller.

At each time step k, the longitudinal (lateral) speed $x_{2,i}(k)$ $\left(x_{4,i}(k)\right)$ of the vehicles i is compared with the corresponding target speed. Then the resulting error $e(k)$ is the input value for the control system. The achieved longitudinal (lateral) target speed force $f^{ts}_{x,i}(k)$ $\left(f^{ts}_{y,i}(k)\right)$ is then used as a part of vehicle dynamics input. i.e., acceleration.

Artificial Potential Fields

The second goal of the driving strategies for CAVs is collision avoidance. In conventional lane-based driving environment, drivers tend to maintain a certain comfort and safety distance from the front vehicles. This depends on the acceptable time gap for the drivers. Hence, the space gap between the vehicles also depends on the vehicles' speed. This prevents rear-end collisions.

In the lane-free environment, we maintain the proper distance between CAVs using artificial potential fields and corresponding inter-vehicle forces. To this end, and to avoid collision, we assume that each vehicle is surrounded by an artificial potential field that applies repulsion or nudging forces to other vehicles within its field. We follow the approach proposed in (*20*), with some modifications, to create the potential functions. First, we assume a safety ellipse around each vehicle j, which acts as an obstacle. The major and minor axes of this ellipse, d_x and d_y respectively, depend on the time-gap-like parameters and the speed of vehicle j and the vehicle i, as defined in Equation 4.

$$d^j_x(k) = s_x l_i + t_{1,x}\left(x_{3,i}(k) + x_{3,j}(k)\right) + t_{2,x}\left|x_{3,i}(k) - x_{3,j}(k)\right| \tag{4a}$$

$$d^j_y(k) = s_y w_i + t_y\left[\tanh\left(\frac{x_{2,i}(k) - x_{2,j}(k)}{x_{4,j}(k) - x_{4,i}(k) + \varepsilon}\right) + \sqrt{\left\{\tanh\left(\frac{x_{2,i}(k) - x_{2,j}(k)}{x_{4,j}(k) - x_{4,i}(k) + \varepsilon}\right)\right\}^2 + \varepsilon}\right] \tag{4b}$$

The first terms in Equation 4a and Equation 4b provide a minimum safety gap between vehicles in the stationary mode where l_i and w_i are the length and width of the vehicle i, respectively, and s_x and s_y are safety factors. The second term in Equation 4a maintains additional space-gaps behind and in front of the obstacle vehicle j. The third term in Equation 4a, takes the relative speeds into account and induces lower space-gaps when two vehicles are driving with the same speed, e.g., in a flock. The lateral ellipse axis depends on the relative lateral speed and distance of two vehicles as represented in the second term in Equation 4b and is applied only if two vehicles are laterally approaching each other as suggested in (*20*). This term implies that the greater the lateral speed deviation or the smaller the lateral space-gap between two vehicles cause larger lateral axis of the ellipse and, hence, a bigger repulsion force. $t_{1,x}$, $t_{2,x}$, and t_y are time gaps which are selected appropriately to provide a collision-free driving behavior. Using the ellipse axes 4, the potential function by which the repulsion and nudging force are calculated is defined as follows:

$$F(i,j,k) = \frac{M}{\left[\left(\frac{x_{1,i}(k)-x_{1,j}(k)}{0.5\cdot d_x^j(k)}\right)^{f_1} + \left(\frac{x_{3,i}(k)-x_{3,j}(k)}{0.5\cdot d_y^j(k)}\right)^{f_2}\right]^{f_3} + 1} \tag{5}$$

where M is the maximum value of the function, f_1 and f_2 are positive even integers and f_3 is a positive integer. The resulting inter-vehicle force from Equation 5 is applied to the front vehicle as the nudging force and to the rear vehicle as a repulsive force and are in the direction of the line connecting two vehicles' centers as shown in Figure 3, where in this representation M equals 2. These forces are then projected into the longitudinal and lateral directions, which are used in 6 for updating the vehicle's acceleration.

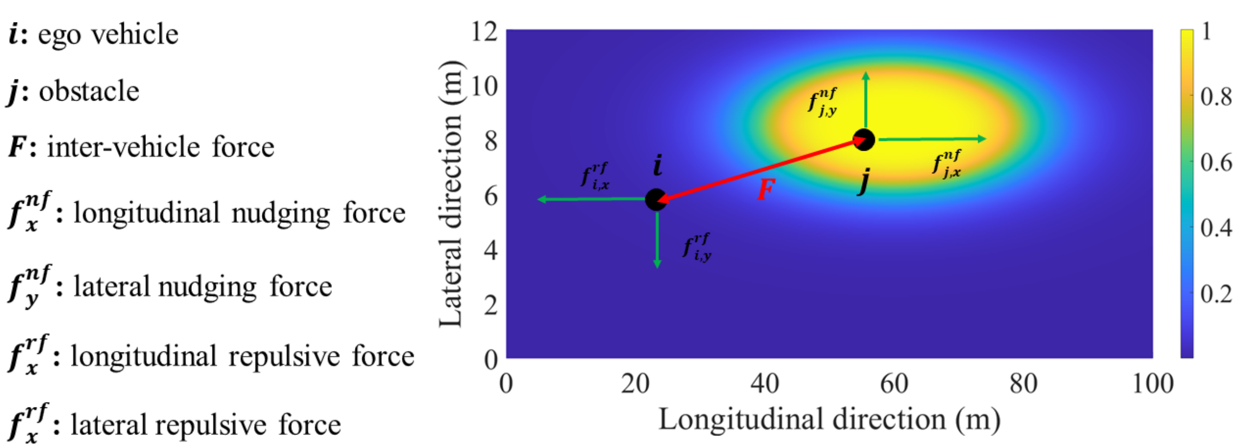

FIGURE 3: The repulsive and nudging forces affect the vehicles' movement.

To achieve the collision avoidance goal, the derived forces are combined with the longitudinal and lateral target speed forces derived from the cruise controller at given discrete time k and are computed via the following respective equations:

$$u_{x,i}(k) = \left[f_{x,i}^{ts}(k) + c_x^{vf} \sum_{j=1}^{J} \left(f_{x,j}^{rp}(k) + c_x^{nf} f_{x,j}^{nf}(k)\right)\right] / m \tag{6a}$$

$$u_{y,i}(k) = \left[f_{y,i}^{ts}(k) + c_y^{vf} \sum_{j=1}^{J} \left(f_{y,j}^{rp}(k) + c_y^{nf} f_{y,j}^{nf}(k) \right) \right] / m \tag{6b}$$

where m is the vehicle mass, c^{vf} and c^{nf} are scalar coefficients that regulate the effect of virtual forces and the nudging force, respectively. f_j^{rp} is the repulsive force and is applied due to vehicle j in front to avoid collision and f_j^{nf} is the nudging force applied from the vehicle j behind and aims to facilitate the advancement of the faster vehicles where J is the total number of neighboring vehicles in the detection zone of the vehicle i. The subscripts x and y in Equation 6 refer to the corresponding coefficients and force in the longitudinal and lateral directions, respectively. In addition to the terms in Equation 6b, there is another force which maintains the lateral location of the vehicles based on their desired speed and is explained in the following section.

Potential lines for lateral distribution of vehicles

In a lane-fee environment, as vehicles can choose any arbitrary lateral location, the relatively intense interactions between CAVs may cause some negative chain effects in the traffic flow. For example, the interactions generated between two CAVs with larger speed differences are more drastic compared to that of two CAVs with smaller speed differences. Such interactions imply greater forces and thus bigger accelerations which lead to speed fluctuations for other vehicles. This condition increases the chaos in the traffic flow and is especially significant at higher vehicle densities. Hence, if CAVs with larger differences in their desired speed are laterally distanced, the mentioned turbulent flow can be weakened to a great extent.

Inspired by the road traffic rules in most countries around the world, where vehicles must overtake from the left side and slow moving vehicles take the right lanes of the road to drive in, we proposed the concept of potential line to uniformly distribute the vehicles across the road width based on their desired speed.

On a given section of the road, for each vehicle i, a potential line $y_{pL,i}(x, v_{x,i}^d)$ is allocated that changes with regards to the vehicle's longitudinal target speed and road geometry. For a vehicle i , at longitudinal coordinate x, its potential line is obtained via the following equation:

$$y_{pl,i}(x, v_{x,i}^d) = \left(Y_{left}(x) - Y_{right}(x) - w_i \right) \frac{v_{x,i}^d - v_{min}^d}{v_{max}^d - v_{min}^d} \tag{7}$$

where $Y_{left}(x)$ and $Y_{right}(x)$ are the left and right boundary functions, respectively. $v_{x,i}^d$ is the longitudinal desired speed of vehicle i, v_{max}^d and v_{min}^d represents the maximum and the minimum desired speeds of all vehicles. A stretch of beltway segment marked with a series of potential lines is illustrated in Figure 4.

The dash lines shown in Figure 4 represent the different potential lines and the color of the dash lines indicates the desired speed to which they correspond. The induced potential lines have the following characteristics:

1. Vehicles with the same longitudinal desired speed v_x^d have the same potential line y_{pl}.
2. The desired speeds corresponding to the potential lines decrease from the left boundary to the right road boundary. Therefore, the leftmost potential line corresponds to the highest desired speed and the rightmost potential line matches the lower desired speed

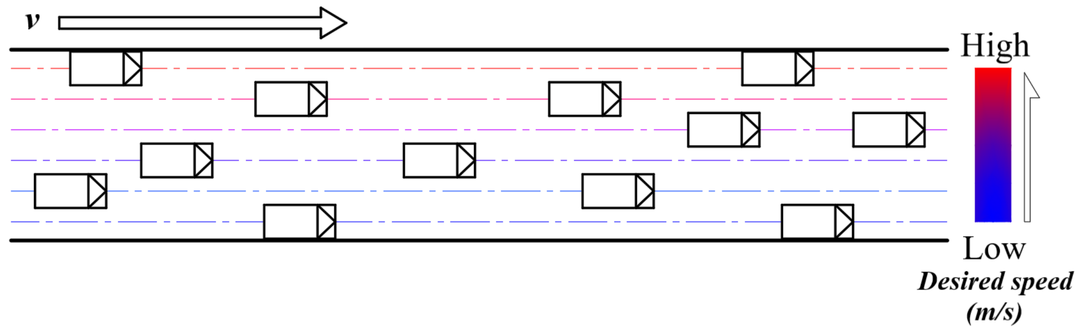

FIGURE 4: Potential lines on a beltway section.

of the CAVs in the section.

3. As the number of the vehicles and their corresponding desired speed is not limited, theoretically there are infinite numbers of the potential lines.

Once the potential line for a vehicle is defined, a corresponding force is calculated and applied laterally on the vehicle to maintain its lateral location. Therefore, when the vehicle i deviates from its potential line $y_{pl,i}$, it will be affected by a lateral force $f_{y,i}^{pl}$ towards its potential line. This force is calculated similar to the cruise controller approach based on the Equation 8.

$$f_{y,i}^{pl}(k) = K_{pl}\big(y_{pl,i}(k) - x_{3,i}(k)\big) \tag{8}$$

where K_{pl} is the controller gain. Using this new force, the Equation 6b will be updated as follows:

$$u_{y,i}(k) = \left[f_{y,i}^{ts}(k) + c_y^{vf} \sum_{j=1}^{J} \left(f_{y,j}^{rp}(k) + c_y^{nf} f_{y,j}^{nf}(k) \right) + f_{y,i}^{pl}(k) \right] / m \tag{9}$$

Hence, the CAVs driving on the road width are laterally kept away from those vehicles that have greater differences in their desired speeds. Furthermore, CAVs driving with potential forces prefer overtaking from the left side and giving way on the right. These features allow vehicles to drive in an orderly manner in a lane-free environment similar to the current lane-based traffic. This approach reduces the chaotic driving behavior of CAVs and leads to much higher throughput as will be shown in the simulation section.

Road boundary control

All the vehicles must remain within the road boundary, i.e, $Y_{right}(x) \leq x_{3,i}(k) \leq Y_{left}(x)$. Therefore, the need for efficient boundary control for the flock is essential. To this end, additional lateral acceleration constraints are required. This task may be addressed as a feedback control problem similar to the cruise controller as shown in Figure 5, where the left (right) road boundary is considered as a reference value for all vehicles' lateral movement and $e(k)$ indicates the error between the current lateral position of the vehicle and the left (right) road boundary (*27*). This control command specifies how much lateral acceleration is needed to lead the vehicle towards the boundary. This value is then assumed as the maximum acceleration and ensures that the vehicles never cross the boundary.

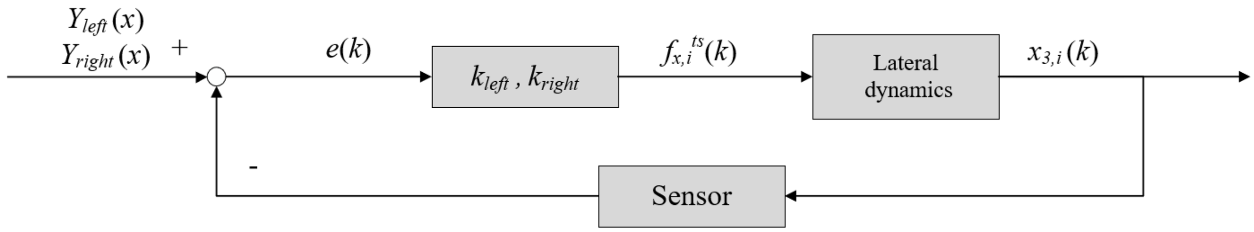

FIGURE 5: Feedback loop for boundary control.

Therefore the lateral bound constraint 2b is updated as follows:

$$u_{y,i}(k) \leq min\left(u_{y,max}(k)\,,\, k_{left}\left(Y_{left}(x) - x_{3,i}(k)\right)\right) \tag{10a}$$

$$u_{y,i}(k) \geq max\left(u_{y,min}(k)\,,\, k_{right}\left(Y_{right}(x) - x_{3,i}(k)\right)\right) \tag{10b}$$

where k_{left} and k_{right} are controller gains for left and right boundaries, respectively.

SIMULATION RESULTS AND DISCUSSIONS

Simulation environment

To test the proposed algorithm, a traffic network is developed in the traffic simulator SUMO (Simulation of Urban Mobility) (*28*). The simulation is executed using a custom extended version of SUMO called TrafficFluid-Sim. It extends the open-source codebase of SUMO to meet the needs of LFT simulation environments (*29*).

An external application programming interface (API) is used for controlling vehicular dynamics and defining vehicle driving strategies. It allows users to set the desired speed of the vehicles, scanning vehicles, getting their states, and defining new longitudinal and lateral acceleration for vehicles in the given time step.

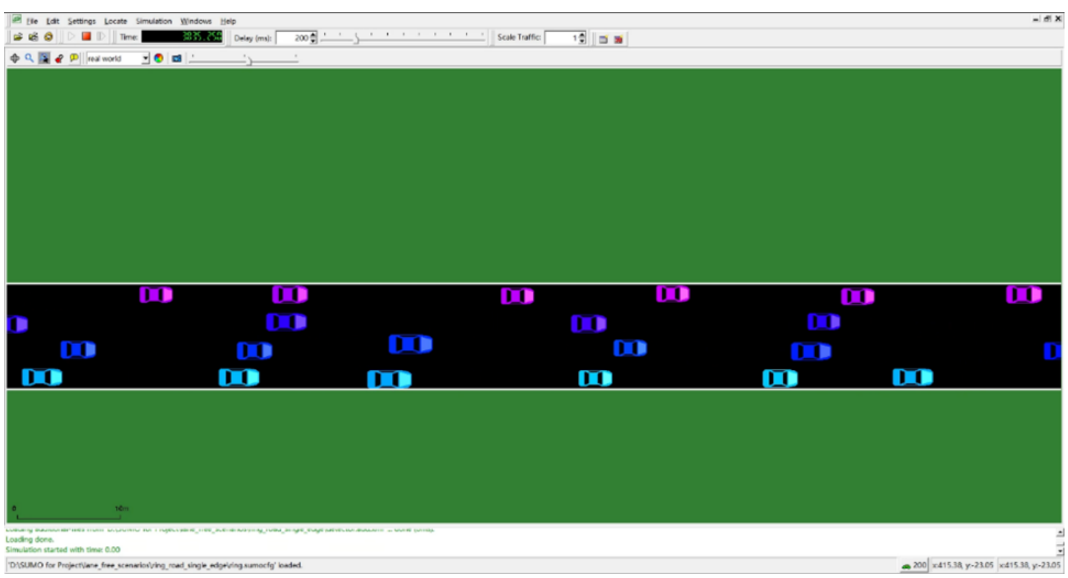

FIGURE 6: Simulation environment.

The considered traffic network is a 1 *km* long freeway. To emulate the beltway effect, we let the vehicles leaving from the end of the network to be entered from the other side of the road at exactly the same lateral position and with the same longitudinal and lateral speeds. Since the goal for this paper is to evaluate the capacity of the beltway in an LFT environment, the width of the beltway is defined based on the considered scenarios. In this work, we define three scenarios; 1- a lane-free beltway as wide as a three-lane conventional beltway, i.e., with the width of 10.2 *m*; 2- half lane reduction of the width, i.e., with the width of 8.5 *m*, and 3- one full lane reduction of the width, i.e., with the width of 7 *m*. In the simulation, five types of vehicles are considered, each with its own dimensions (length, width) in meters: (3.2, 1,6), (3.3, 1.7), (3.4, 1.7), (3.5, 1.8), (3.6, 1.82). A snapshot of the developed traffic network is shown in Figure 6, where different sizes of vehicles and the lane-free feature are evident. At each scenario, the distribution of the vehicle types is considered fixed with ratios of [0.27 0.23 0.20 0.17 0.13].

Results and discussion

For each scenario, we run simulations with various density of vehicles starting from 50 veh/km. The maximum density of each scenario depends on the limitation of the beltway capacity. The maximum densities are 250, 350, and 450 veh/km for scenario 1, 2, and 3, respectively. Vehicles are identically inserted at simulation time 0 s with an initial speed of 0 m/s in both lateral and longitudinal directions. The vehicles are also positioned within the considered road boundaries. Each vehicle is equally assigned with a predefined desired speed in the range of 25 to 35 m/s. Each scenario is simulated for 20 minutes.

In Figure 7, the fundamental diagram for each scenario is illustrated. It reveals the fact that the capacity of the 10.2 *m* beltway is around 30000 veh/h which is much higher than the equivalent lane-based beltway. In addition, comparing this flow with similar LFT strategies ((*15, 27*)) show that the implementation of the potential field approach considerably affects the throughput of a lane-free road. As one may expect, with road narrowing, the capacity of the beltway decreases accordingly. The important point is that, even in the third scenario, where the road is as wide as a conventional two-lane road, the maximum flow is higher than the original three-lane road. This finding is crucial and highlights the effectiveness of lane-free traffic.

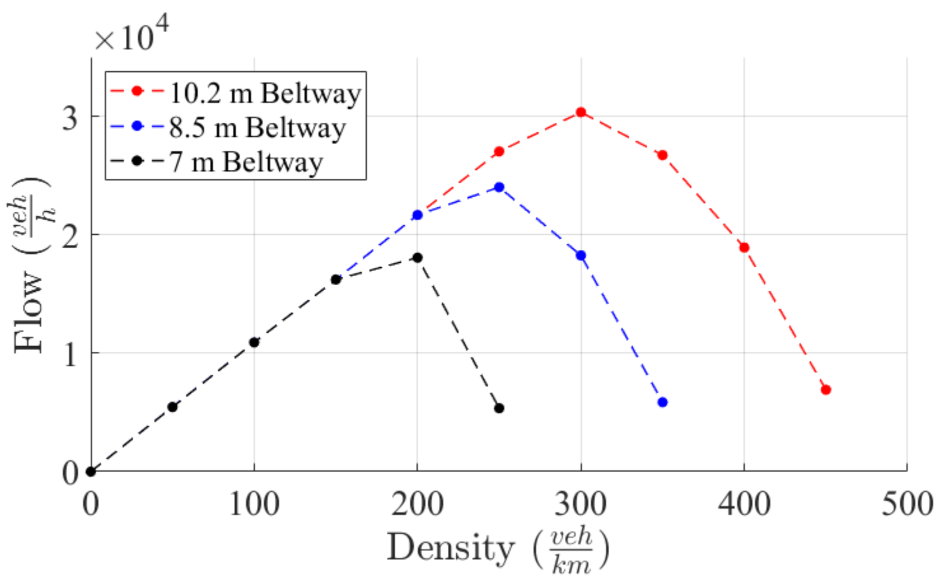

FIGURE 7: Fundamental diagrams for the three scenarios

However, once we change the width of the considered beltway, the corresponding flows and densities are affected, especially in the congested situation. To have a uniform comparison of a fundamental diagram regardless of the road width, we suggest to normalize the flow and densities with respect to the road width.

$$q_n = \frac{q}{R_w} \tag{11a}$$

$$\rho_n = \frac{\rho}{R_w} \tag{11b}$$

In (11), q and ρ are the common flow and density, whereas, q_n and ρ_n are the normalized flow and densities, respectively. The new normalized fundamental diagrams with the new definition of flow and density is shown in Figure 8.

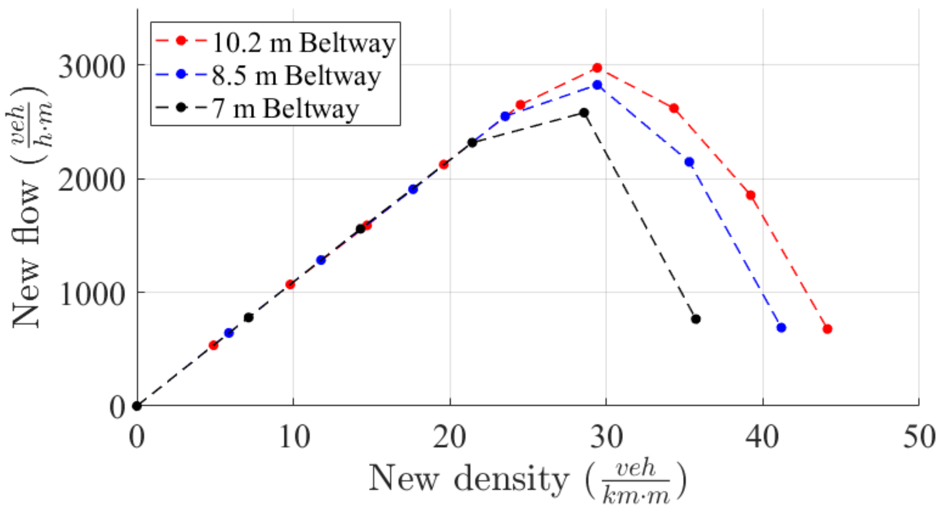

FIGURE 8: Normalized fundamental diagrams for the three scenarios

The diagrams in Figure 8 show that different scenarios demonstrate relatively a similar critical density and maximum flow. In addition, the wider the road the higher the normalized density. This fact indicates that LFT is highly effective on wider roads, where vehicles have more freedom for lateral movement. In other words, the lateral occupancy of the wider roads in congested situations are higher, compared to narrower roads.

To have a better insight on the designed potential lines, the lateral trajectories of three random selected vehicles at each scenario are plotted in Figure 9. Each vehicle is initiated at a random lateral location whereas it receives a potential line at a different lateral location due to its desired speed. Just after a few seconds, all vehicles reaches their assigned lateral location, i.e., their potential lines, and keep such lateral locations in the rest of the simulation run. However, the vehicles may deviate at some point from their desired lateral positions due to the inter-vehicle forces. But it is important to see that they try to maintain their positions regardless of the applied forces.

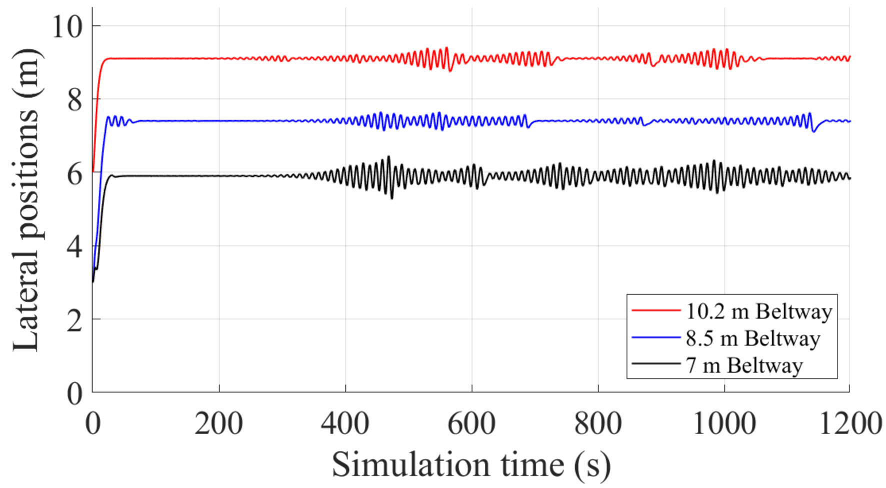

FIGURE 9: Lateral movement of three selected vehicles

In order to evaluate the behavior of the vehicles, the speed and acceleration of three vehicles in each scenario are shown in Figure 10-12. The longitudinal speeds show that all vehicles reach their desired speed and the speed is maintained for the rest of the simulation run. The acceleration phase in the narrower road (Figure 12) is longer since the interference of the vehicles is higher. Therefore, it takes more time for the vehicle to reach its desired speed. The lateral speed diagrams also demonstrates the fact that all the vehicles initially take a lateral speed to align themselves with their potential lines. Following the initial phase, the lateral speed fluctuates around zero.

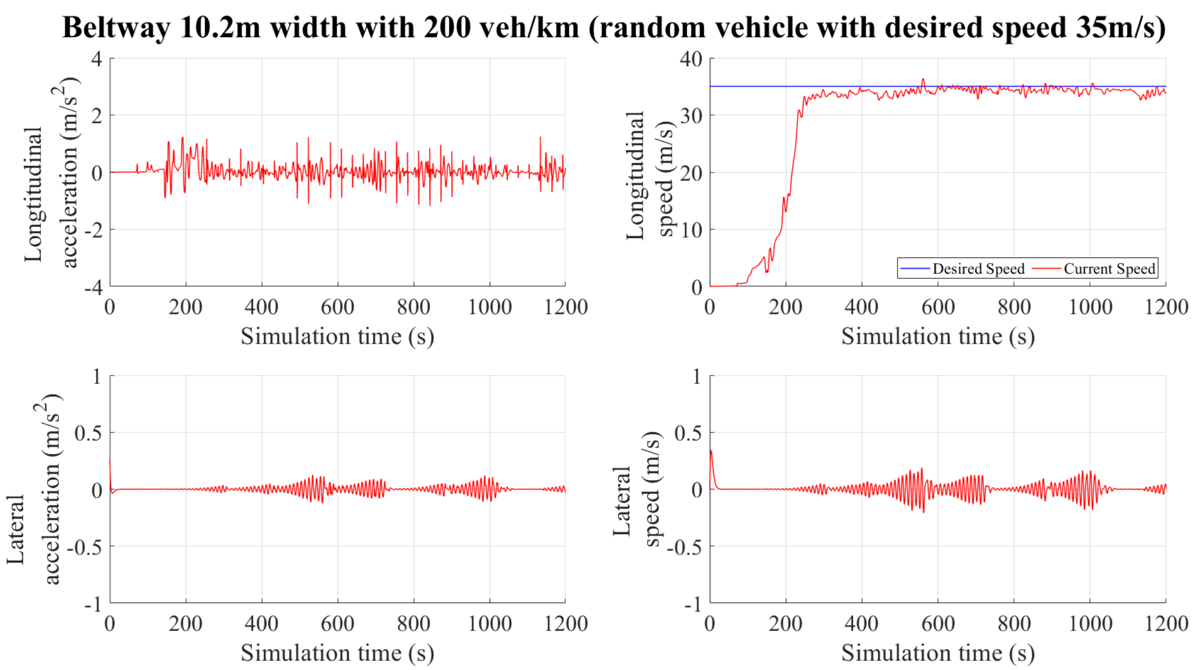

FIGURE 10: Acceleration and speed of a vehicle in 10.2 *m* scenario

The lateral and longitudinal speed fluctuation on the wider road is less than the narrower ones. This issue is predictable as vehicles, with similar densities, on a wider road have more freedom to maneuver. However, the lateral acceleration of all selected vehicles are less than 0.5 m/s^2 which fulfills comfort considerations of CAV driving strategy.

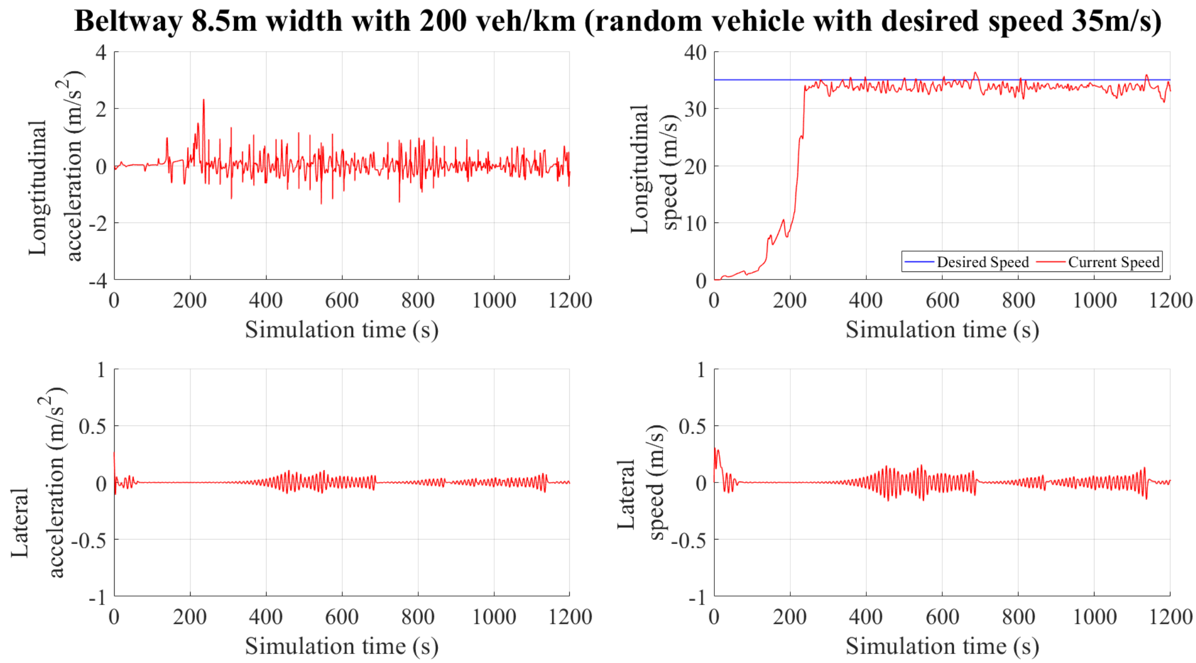

FIGURE 11: Acceleration and speed of a vehicle in 8.5 *m* scenarios

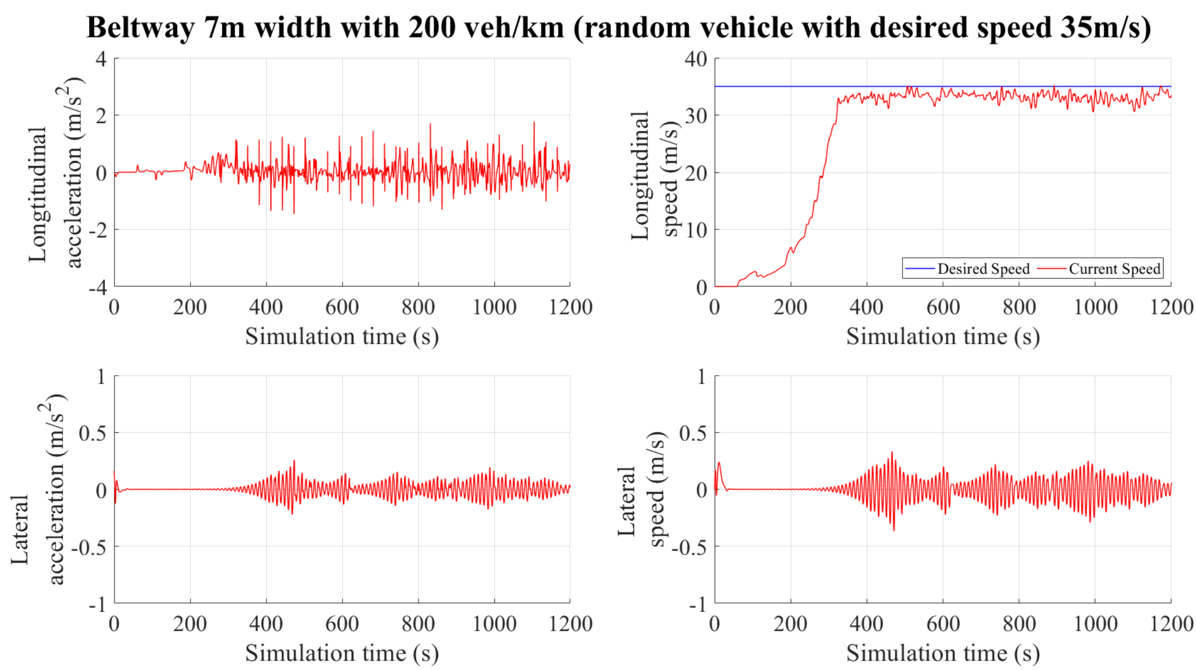

FIGURE 12: Acceleration and speed of a vehicle in 7 *m* scenarios

In summary, by adopting lane-free traffic with potential lines as a vehicle driving strategy, we show that the width of the beltway can be shrunk appropriately to save land resources without losing road capacity. The extra resources may be more efficiently used by other road users such as cyclists or public transportation. At the same time, this idea satisfies not only capacity requirements but also comfort considerations.

To further investigate the safety and comfort issues associated with the designed lane-free driving strategy, we placed a virtual detector at the leftmost section of the road, i.e., at the longitudinal location of the 940 *m* and the lateral location covering the lateral width of the road between 8.4 and 10.2 *m*. This detector measures the speed, space-gap, and time-gap of the passing vehicles. Due to the designed potential lines and the location of the detector, we expect that this detector measures the variables associated with fast-moving vehicles. The average space-gap and time-gap between vehicles and the average speed at different scenarios are recorded and shown in Figures 13-15.

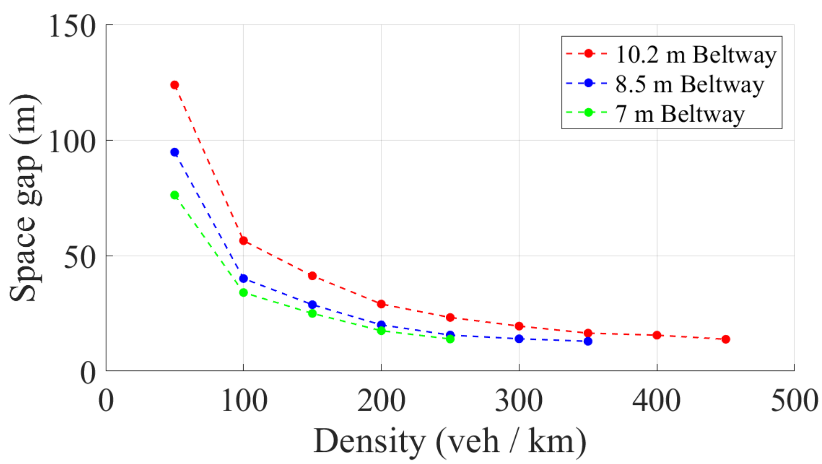

FIGURE 13: Space-gap diagram

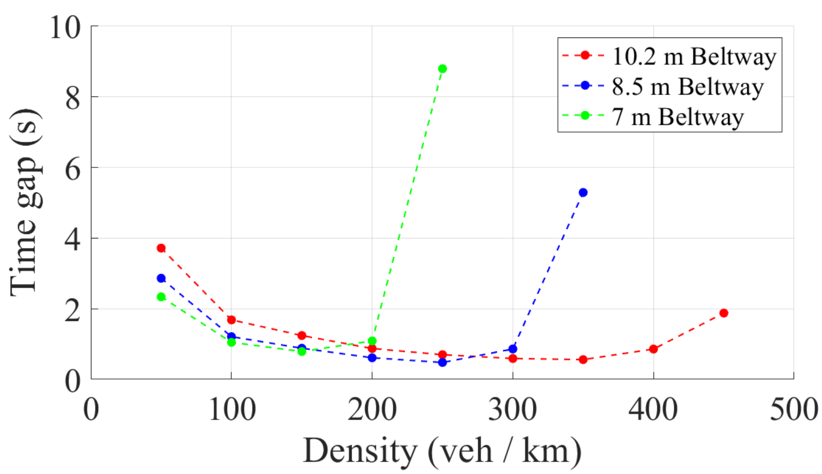

FIGURE 14: Time-gap diagram

It can be seen that the space and time gaps between vehicles decreases as the density increases. However, after the critical density, as the speed of the vehicles starts to reduce, the corresponding time-gap increases. The shortest space-gap between vehicles is around 10 *m* and the shortest time-gap is about 0.5 *s*.

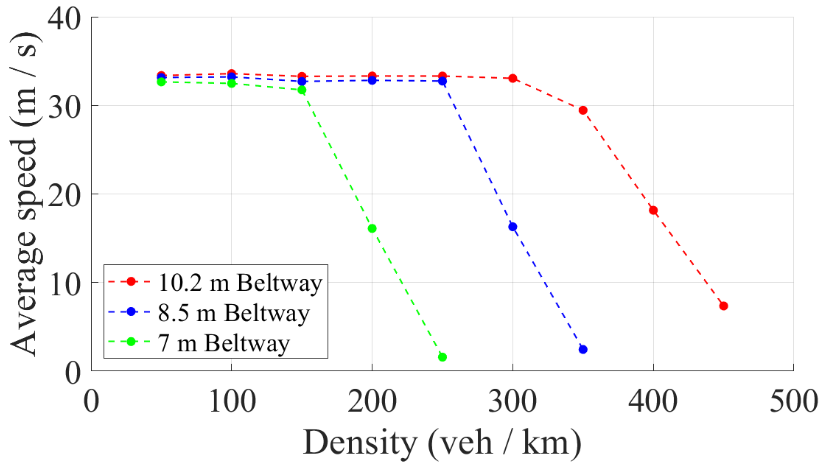

FIGURE 15: Average speed

CONCLUSION AND FUTURE WORKS

In this paper we developed a new approach to further increase road capacity on lane-free beltways by using potential lines. In the lane-free traffic environment, the throughput is higher compared to the lane-based conventional traffic systems. However, with the proposed approach, due to the harmonic lateral distribution of the vehicles across the road width, the achieved flow and densities are considerably higher than already available lane-free driving strategies.

The simulation results show, even for the cases where we reduced the road width, we observe a comparable capacity to lane-based traffic with full width. In addition, the results also show that the potential lines allow vehicles to drive at a speed closer to the predefined desired speed even at a very high traffic demand, resulting in no delay time. This is indeed a great achievement and implies that to resolve road congestion, we can do away with constructing new roads or extending existing one.Rather by exploiting CAV technology, the capacity of the current road infrastructure will be maximized. In addition, we propose that, with regards to high capacity of the lane-free roads, the width of the current roads can be reduced and the remaining road space can be allocated to other road users such as cyclists or for public transport.

In future works, we aim to focus on the safety and comfort aspects of LFT. Although this speed-dependent lateral distribution leads to very high throughput, the smoothness of the vehicle trajectories and safety analysis must be carefully taken into account. To this end, future works will test such driving strategies in a driving simulator. In addition, it is also important to consider the measurement or communication error and to investigate how they may affect the designed control algorithms. The potential lines could also be combined with flocking, i.e., a group of vehicles driving together with the same speed. In the future, advanced control theories could also be used for diminishing the transition of shock waves by reducing the fluctuation of vehicle dynamics.

ACKNOWLEDGEMENTS

This work is based on the project "Simulation and organization of future lane-free traffic" funded by the German research foundation (DFG), under the project number BO 5959/1-1.

AUTHOR CONTRIBUTIONS

The authors confirm contribution to the paper as follows. Study conception: M. Rostami-Shahrbabaki, H. Zhang, M. Sekeran; methodology development: M. Rostami-Shahrbabaki, H. Zhang; implementation and simulation: H. Zhang; Analysis and interpretation of results: M. Rostami-Shahrbabaki; draft manuscript preparation: M. Rostami-Shahrbabaki, H. Zhang, M. Sekeran, K. Bogenberger; All authors reviewed the results and approved the final version of the manuscript.

REFERENCES

1. Baum-Snow, N., L. Brandt, J. V. Henderson, M. A. Turner, and Q. Zhang, Roads, Railroads, and Decentralization of Chinese Cities. *The Review of Economics and Statistics*, Vol. 99, No. 3, 2017, pp. 435–448.
2. Ishikura, T. and F. Yokoyama, Regional economic effects of the Ring Road project in the Greater Tokyo Area: A spatial CGE approach. *Papers in Regional Science*, 2022.
3. Zhiyuan, G. and Z. Fucheng, Study on the Traffic Impact Analysis of the Second Ring Road in Beijing. In *2009 Second International Symposium on Information Science and Engineering*, 2009, pp. 505–508.
4. Nugmanova, Arndt, Hossain, and Kim, Effectiveness of Ring Roads in Reducing Traffic Congestion in Cities for Long Run: Big Almaty Ring Road Case Study. *Sustainability*, Vol. 11, No. 18, 2019, p. 4973.
5. Burton, R. C. and F. D. Knapp, SOCIO-ECONOMIC CHANGE IN VICINITY OF CAPITAL BELTWAY IN VIRGINIA. *Highway Research Record*, 1964.
6. Blinnikov, M., A. Shanin, N. Sobolev, and L. Volkova, Gated Communities of the Moscow Green Belt: Newly Segregated Landscapes and the Suburban Russian Environment. *GeoJournal*, Vol. 66, No. 1, 2006, pp. 65–81.
7. Kijowska, J. and A. Kijowski, Landscape changes caused by the construction of the Poznań western ring road – selected problems to their potential applications. *Teka Komisji Ochrony I Kształtowania Środowiska Przyrodniczego*, Vol. Vol X, 2013.
8. Janas, M. and A. Zawadzka, Analysis of the Impact of the Eastern Ring Road of Lodz on Selected Components of the Environment. *E3S Web of Conferences*, Vol. 28, 2018, p. 01014.
9. Morello, E., S. Manfredi, and A. Matassi, MARCO (Motorway Access Regulation and Control)-An Innovative Integrated Freeway Management System On Venice Beltway. In *Proceedings of the 7th World Congress on Intelligent Transport Systems held in Turin, Italy 6.9 NOVEMBER*, 2000.
10. Nohekhan, A., S. Zahedian, and K. F. Sadabadi, Investigating the Impacts of I-66 Inner Beltway Dynamic Tolling System. *Transportation Engineering*, Vol. 4, 2021, p. 100059.
11. Bogenberger, K. and A. D. May, Advanced Coordinated Traffic Responsive Ramp Metering Strategies, 1999.
12. Johansen, S. I. and A. S. Løvland, *Flocking for Road Traffic Efficiency Improvement-A Concept Study*. Master's thesis, NTNU, 2015.
13. Papageorgiou, M., K.-S. Mountakis, I. Karafyllis, I. Papamichail, and Y. Wang, Lane-free artificial-fluid concept for vehicular traffic. *Proceedings of the IEEE*, Vol. 109, No. 2, 2021, pp. 114–121.
14. Sekeran, M., M. Rostami-Shahrbabaki, A. A. Syed, M. Margreiter, and K. Bogenberger, Lane-Free Traffic: History and State of the Art. In *2022 IEEE International Intelligent Transportation Systems Conference (ITSC)*, 2022, p. 6, submitted.
15. Berahman, M., M. Rostmai-Shahrbabaki, and K. Bogenberger, Driving Strategy for Vehicles in Lane-Free Traffic Environment Based on Deep Deterministic Policy Gradient and Artificial Forces. *IFAC-PapersOnLine*, Vol. 55, No. 14, 2022, pp. 14–21.
16. Troullinos, D., G. Chalkiadakis, I. Papamichail, and M. Papageorgiou, Collaborative multiagent decision making for lane-free autonomous driving. In *Proceedings of the 20th In-*

ternational Conference on Autonomous Agents and MultiAgent Systems, 2021, pp. 1335–1343.

17. Studer, L., M. Cecchetto, G. Marchionni, and M. Ponti, *Evaluation of Dynamic Speed Control on the Venice-Mestre Beltway*, 2009.
18. Jang, K. and M. J. Cassidy, Dual Influences on Vehicle Speed in Special-Use Lanes and Critique of US Regulation. *Transportation Research Part A: Policy and Practice*, Vol. 46, No. 7, 2012, pp. 1108–1123.
19. Li, W.-T., J.-Q. Li, B.-K. Chen, X. Huang, and Z. Wang, Information Feedback Strategy for Beltways in Intelligent Transportation Systems. *EPL (Europhysics Letters)*, Vol. 113, No. 6, 2016, p. 64001.
20. Yanumula, V. K., P. Typaldos, D. Troullinos, M. Malekzadeh, I. Papamichail, and M. Papageorgiou, Optimal path planning for connected and automated vehicles in lane-free traffic. In *2021 IEEE International Intelligent Transportation Systems Conference (ITSC)*, IEEE, 2021, pp. 3545–3552.
21. Levy, R. and J. Haddad, Path and Trajectory Planning for Autonomous Vehicles on Roads without Lanes. In *2021 IEEE International Intelligent Transportation Systems Conference (ITSC)*, IEEE, 2021, pp. 3871–3876.
22. Karafyllis, I., D. Theodosis, and M. Papageorgiou, Two-dimensional cruise control of autonomous vehicles on lane-free roads. *arXiv preprint arXiv:2103.12205*, 2021.
23. Malekzadeh, M., I. Papamichail, M. Papageorgiou, and K. Bogenberger, Optimal internal boundary control of lane-free automated vehicle traffic. *Transportation Research Part C: Emerging Technologies*, Vol. 126, 2021, p. 103060.
24. Malekzadeh, M., I. Papamichail, and M. Papageorgiou, Linear–Quadratic regulators for internal boundary control of lane-free automated vehicle traffic. *Control Engineering Practice*, Vol. 115, 2021, p. 104912.
25. Chavoshi, K. and A. Kouvelas, Distributed control for laneless and directionless movement of connected and automated vehicles. In *21st Swiss Transport Research Conference (STRC 2021)*, STRC, 2021.
26. Rostami-Shahrbabaki, M., S. Weikl, M. Akbarzadeh, and K. Bogenberger, A two-layer approach for vehicular flocking in lane-free environment. In *11th Triennial Symposium on Transportation Analysis conference (TRISTAN XI)*, 2022.
27. Malekzadeh, M., D. Manolis, I. Papamichail, and M. Papageorgiou, Empirical Investigation of Properties of Lane-free Automated Vehicle Traffic. In *2022 IEEE International Intelligent Transportation Systems Conference (ITSC)*, IEEE, 2022.
28. Behrisch, M., L. Bieker, J. Erdmann, and D. Krajzewicz, SUMO–simulation of urban mobility: an overview. In *Proceedings of SIMUL 2011, The Third International Conference on Advances in System Simulation*, ThinkMind, 2011.
29. Troullinos, D., G. Chalkiadakis, D. Manolis, I. Papamichail, and M. Papageorgiou, Lane-free microscopic simulation for connected and automated vehicles. In *2021 IEEE International Intelligent Transportation Systems Conference (ITSC)*, IEEE, 2021, pp. 3292–3299.